

NASA Technical Memorandum 4409

Application of Laser Doppler Velocimeter to Chemical Vapor Laser System

(NASA-TM-4409) APPLICATION OF
LASER DOPPLER VELOCIMETER TO
CHEMICAL VAPOR LASER SYSTEM (NASA)
22 p

N93-18068

Unclass

H1/36 0145558

Luther R. Gartrell
Langley Research Center
Hampton, Virginia

Bagher M. Tabibi
Hampton University
Hampton, Virginia

William W. Hunter, Jr., Ja H. Lee,
and Mark T. Fletcher
Langley Research Center
Hampton, Virginia



National Aeronautics and
Space Administration
Office of Management
Scientific and Technical
Information Program
1993

Acknowledgment

The authors wish to acknowledge R. C. Costen and W. E. Meador of the Space Systems Division for suggesting and initiating the application of laser velocimetry for this work. In addition, the authors acknowledge C. E. Nichols, Jr., of the Facilities Engineering Division for his assistance with the design of the seeding system.

Use of Trademarks

The use of trademarks or names of manufacturers in this report is for accurate reporting and does not constitute an official endorsement, either expressed or implied, of such products or manufacturers by the National Aeronautics and Space Administration.

Summary

A laser Doppler velocimeter (LDV) system has been used to measure iodide vapor flow fields within 20- and 36-mm-inside diameter (id) laser tubes used for a solar-simulated, pumped laser system. The velocity profiles across the laser tubes were obtained with an estimated ± 1 -percent bias and ± 0.3 - to 0.5 -percent random uncertainty in the mean values and ± 2.3 -percent random uncertainty in the turbulence-intensity values. For the velocity profile measurements in the 20-mm-id laser tube, the centerline velocities and turbulence intensities for various longitudinal locations ranged from 13 to 17.5 m/sec and 6 to 20 percent, respectively. These measurements showed that the level of turbulence was higher than generally anticipated. Therefore, modeling of the flow field should include considerations for the effects of turbulence. For the 36-mm-id tube, the centerline velocity at the length/diameter (l/d) = 24 location was 11 m/sec with an 8-percent turbulence-intensity level. The LDV system provided calibration data for pressure and mass flow systems used routinely to monitor the chemical laser gas flow velocity. When the estimated average velocity values derived from the LDV mean centerline velocities and the "pipe factor" were compared with pressure and mass flow measurements, agreement was within 6 percent. The LDV system has provided flow velocity data for use in calibrating the installed instrumentation and for analyzing the flow characteristics of perfluoroalkyl iodide ($n\text{-C}_3\text{F}_7\text{I}$) vapor inside various laser tubes.

Introduction

Feasibility studies of high-power laser systems for space applications are being conducted at the Langley Research Center (LaRC). The focus of the present activity is a solar-simulated, pumped gas laser that can deliver continuous wave (cw) power of about 10 W using thermally driven normal perfluoroalkyl iodide ($n\text{-C}_3\text{F}_7\text{I}$) vapor (ref. 1). The photodissociation of the flowing iodide vapor inside a transparent quartz laser tube is produced by a "vortex-stabilized" argon arc light source. Vapor flow studies were needed to assess the impact of flow-field characteristics on laser operating efficiency and for validation of a numerical model formulated for the laser system.

A laser Doppler velocimeter (LDV) was selected to measure the vapor flow-field characteristics because it is nonintrusive and has been successfully applied to a variety of fluid dynamics applications (refs. 2 to 5). The LDV measures particle velocities in the moving fluid. Through selective control of particle size to reduce particle lag, particle velocity can be equated with the fluid velocity within the accuracy of the LDV system. Real-time absolute LDV measurements are obtained independent of local fluid conditions except for the dependence of particle dynamic response on local flow-field temperature and pressure.

This paper describes the LDV experiments conducted to determine flow characteristics in two different sizes of transparent laser tubes. The pipe flow experiments also provided data to assess the performance of the pressure and mass flowmetering systems that are used routinely to monitor the research laser system. The LDV measurement technique, test apparatus, procedure, and results are described.

Symbols

A	laser tube cross-sectional area, cm^2
b	linear regression intercept
d	laser tube inside diameter, cm
F	mass flow rate, SCCM
f_c	reference clock frequency, Hz

f_D	Doppler frequency, Hz
l	longitudinal distance, mm
m	slope of linear regression curve fit
P	laser tube pressure, torr
q	defined nondimensional quantity, equation (6)
SCCM	standard cubic centimeters per minute
V	velocity, m/sec
\bar{V}	estimated average velocity, m/sec
V_c	calculated velocity, m/sec
V_m	measured velocity, m/sec
x	radial distance, figures 8 and 9
γ	turbulence intensity, σ/V
ΔV	velocity uncertainty, m/sec
$\Delta\theta$	measured crossbeam angle uncertainty, rad
ϵ_γ	error in turbulence intensity
ϵ_V	error in mean velocity
θ	angle between intersecting laser beams, deg
λ	laser wavelength, nm
σ	standard deviation of velocity, m/sec
σ_m	standard error of statistical mean, m/sec
σ_s	standard error of standard deviation, m/sec

Laser Doppler Velocimeter Technique

The underlying principles of the LDV technique are embodied in Maxwell's equations and the Doppler effect. A solution for Maxwell's equations was developed by Mie (discussed in ref. 6) that describes the properties of electromagnetic fields scattered from a homogeneous sphere, denoted Mie scattering. The Doppler frequency shift of the scattered radiation is shown in figure 1, where a pair of laser beams cross to form a sample volume. Particles passing through that volume will scatter light at a Doppler-shifted frequency that is proportional to the velocity of the scattering particle normal to the crossbeam angle bisector. The Doppler frequency is given by

$$f_D = \frac{2V \sin\left(\frac{\theta}{2}\right)}{\lambda} \quad (1)$$

where V is the velocity of the particle, θ is the angle between the intersecting beams, and λ is the wavelength of the laser light.

Apparatus

Laser Doppler Velocimeter System

The LDV was a single-component, conventional crossbeam system configured to operate in the forward-scattering mode. A helium-neon laser operating in the TEM_{00} mode provided 15 mW

of continuous power at 623.8 nm. The transmitting optics consisted of a 50:50 beam splitter and a 2.27 \times beam expander that formed two 2.27-mm-diameter, 50-mm spaced parallel beams. The two parallel beams passed through a 105-mm focal length lens and produced a focused crossover point shaping a 36- μ m-diameter by 100- μ m-long elliptical measurement volume. The crossbeam angle was 26.78°. Scattered light was collected by the objective lens of a 2.27 \times optical expander identical to that used in the transmitter system. The expander formed a collimated beam of the collected light, passed it through the 40-mm aperture of a 200-mm focal length lens, and focused it on a 200- μ m-diameter pin hole set before a photomultiplier. The transmit and receive optical systems were mounted on a scan rig that had a 1.0- μ m positioning resolution. (See fig. 2.) In the final optical arrangement, the measurement volume was positioned in a horizontal plane that passed through the axis of the cylindrical research laser tube.

The electronics system that is shown in figure 3 consisted of a frequency-burst counter, microcomputer, printer, and miscellaneous electronics. The frequency-burst counter, a real-time processor that measures the period of Doppler frequency with 1.0-ns resolution, has an input frequency range capability of 1 kHz to 150 MHz. It was equipped with bandpass filters, double-threshold zero-crossing detectors, and comparison circuitry for extraneous noise rejection. This signal processor provides a digitized output of the measured frequency, which is processed with the microcomputer. The resulting velocity information is stored on a disk.

Perfluoroalkyl Iodide Vapor System

The experimental setup for the cw perfluoroalkyl iodide laser system with continuous flow is shown in figure 4. To maintain an efficient operating system, the quenching products that formed because of photodissociation of the iodide vapor in the pumping region were purged from the laser tube. The vapor flow was maintained by a pressure differential between a heated evaporator that contains liquid iodide and a liquid nitrogen-cooled condenser. Perfluoroalkyl iodide is in a liquid state at room temperature and has a vapor pressure of 350 torr; to ensure a sufficient flow rate of iodide, the evaporator was immersed in a tub of heated water and stirred with a magnetic stirrer. The temperature of the water was kept constant at 40°C to provide an initial vapor pressure of about 101 kPa. Before the lasant chemicals were inserted, the laser tube, evaporator, and condenser were evacuated with a diffusion pump that was equipped with a liquid nitrogen trap. A mass flowmeter, connected between the evaporator and the laser tube, was used to monitor the iodide vapor flow rate, which was controlled by an in-line valve between the flowmeter and the evaporator. The averaged flow velocity was calculated by

$$V = 0.127 \frac{F}{AP} \quad (2)$$

where F is the mass flow rate in standard cubic centimeters per minute (SCCM), A is the laser tube cross-sectional area in centimeters squared, P is the laser tube iodide vapor pressure in torr, and V is the velocity in meters per second. The numerical constant (0.127) is the result of unit conversion. When the valve opening is left fixed, the mass flow rate of the iodide vapor is a linear function of the laser tube pressure. This linear progression indicates that the velocity of the vapor in the laser tube remained constant for different flow rates. Therefore, the flow velocity was varied by another valve located downstream between the laser tube and the condenser.

Two different Suprasil-grade quartz laser tubes were used in these experiments; they measured 20 and 36 mm inside diameter (id) by 900 mm long. Stainless steel tubes were used in the flow lines between the laser tube ends, evaporator, and condenser. These flow line tubes were 900 mm long by 12.7 mm id and were connected to the laser tube at approximately 45° to the flow axis. This arrangement was used to achieve nearly axial flow.

Seeding System

During the lasing process, iodide particles are formed in the vapor flow. In initial experiments, we attempted to use these naturally occurring particles as the light-scattering media for the LDV measurements. However, this scheme failed because not enough scattering material of a sufficient size was present for the LDV to operate.

Adequate signals for flow velocity measurements required the iodide vapor flow to be artificially seeded. The seeding system that is shown in figure 5 consists of two micromesh sieve sections, a seed material reservoir, and a control valve. Aluminum oxide (Al_2O_3) particles were used as the seeding material. The supplier classifies the size of the material based on its crystal structure; the $0.3\text{-}\mu\text{m}$ material used in these tests was hexagonal.

The seeder was evacuated to about 10 torr by an external vacuum-pumping system. After the evacuation, the seeder valve was closed to maintain the reduced pressure inside the seeder. Next, the seeder was connected to the iodide vapor flow line, and the iodide flow was brought to the needed pressure by adjustments to the valves in the flow line. When the operating pressure was established and the flow conditions were recorded, the seeder valve was opened and Al_2O_3 particles were gravity fed into the flow. The electromechanical vibrator was used to maintain a constant feed of particles.

Error Analysis

Because the LDV measures the velocity of individual particles, the accuracy of the measurement depends on how well these particles track the flow. The severity of the particle lag depends on the particle mass density, size, and local flow conditions. Because the velocities were low, the lag error was assumed to be negligible.

Other error sources were derived from the optical system, the electronics system, and the measurement uncertainties due to the statistics of the velocity ensemble. The principal error source in the optical system is from the crossbeam angle measurement uncertainty. This uncertainty yields a bias error that can be expressed as

$$\frac{\Delta V}{V} = \cot\left(\frac{\theta}{2}\right) \Delta\theta \quad (3)$$

where θ is the angle between the intersecting beams along the optical axis in degrees and $\Delta\theta$ is the uncertainty of the measured angle expressed in radians. For a crossbeam angle of $26.78^\circ \pm 0.13^\circ$ the bias error in velocity attributed to the uncertainty in angle is ± 1.0 percent.

An additional, potentially significant optical system error occurs when the crossover and focal points of the beams do not converge at the same location. This optical error results in a negative bias in the final mean velocity value (ref. 7). Based on the method given in reference 7 and assuming a worst case situation where the pair of beam focal points and the crossover point are displaced 10 mm, the estimated bias error is -0.6 percent.

For the electronics system, two other significant error sources (refs. 8 and 9) must be considered. These errors are frequency dependent, are associated with the electronic burst-counter signal processor, and are attributable to counter clock synchronization and quantizing. Clock synchronization error occurs when the randomly occurring Doppler frequency is mismatched to the start cycle of the counter internal "free-running" reference clock. This bias error is caused by a 1-clock-count uncertainty in the total measured period of the input Doppler frequency. Quantizing errors occur because the digitizing process of the period for a fixed number of Doppler

cycles has an uncertainty of 1 clock count. An estimate of velocity ϵ_ν and turbulence-intensity errors ϵ_γ from these sources is given by

$$\epsilon_\nu = \frac{q}{2}(1 + \gamma^2) \pm \frac{q^2}{3}(1 + 3\gamma^3) \quad (4)$$

$$\epsilon_\gamma = \frac{q}{2}(1 - \gamma^2) + \frac{q^2}{6\gamma^2} \quad (5)$$

where

$$q = \frac{f_D}{N f_c} \quad (6)$$

γ turbulence intensity

N number of Doppler cycles

f_c reference clock frequency

f_D Doppler frequency

For example, consider a flow condition encountered during these tests; that is, the mean velocity flow was 16.5 m/sec with a 5- to 20-percent turbulence-intensity range. This condition produces a 12.2-MHz mean Doppler frequency. The test system had a signal-processing counter operating with a 1-GHz reference clock and an 8-Doppler-cycle count requirement. The estimated errors for this test situation are $\epsilon_\nu = 0.08$ percent and $\epsilon_\gamma = 0.09$ percent.

The measurement results were based on the statistical mean and the standard deviation of an ensemble of individual scattering events, where each velocity ensemble consists of 1000 scattering events. The standard error of the velocity mean and the standard deviation provide a measure of the uncertainty in the given results. A typical ensemble gave the following standard errors of the mean and standard deviation:

For the 20-mm-id laser tube with $l/d = 35$,

$$\sigma_m = 0.2 \text{ to } 0.4 \text{ percent}$$

$$\sigma_s = 2.2 \text{ percent}$$

For the 36-mm-id laser tube with $l/d = 24$,

$$\sigma_m = 0.2 \text{ to } 0.8 \text{ percent}$$

$$\sigma_s = 2.2 \text{ percent}$$

In summary, the mean velocity values have an estimated +0.4 to -1.6 percent bias and ± 0.3 to 0.9 percent random uncertainties. The turbulence-intensity values have an estimated ± 2.3 percent uncertainty.

Results and Discussion

Flow Velocity Profile Measurements

Velocity and turbulence-intensity profile measurements were made in the 36- and 20-mm-id tubes at operating pressures of 5.0 ± 0.1 and 9.7 ± 0.2 torr, respectively. Because access to the

36-mm-id laser tube was limited, velocity profile data were obtained at one axial location, $l/d = 24$, which is referenced to the iodide vapor inlet (fig. 6). For the 20-mm-id laser tube, LDV measurements were made at various axial locations, as shown in figure 7. Because of the flow system characteristics, the iodide vapor that entered the laser tube expanded, which caused the flow to separate from the tube wall and to form eddies. During that process, the local flow velocity was abruptly reduced and the resulting flow velocity profile became asymmetric and highly turbulent. This effect is evident in the profiles in figure 8. Velocity measurements at the downstream location $l/d = 4.5$ near the wall opposite the iodide vapor inlet (+0.75-cm position in fig. 7(a)) were not obtained because the flow was separated and no particles were entrained there. However, complete flow velocity profiles at ± 0.75 cm about the centerline were obtained further downstream as the flow became more structured and less turbulent.

Typical histograms of the velocity data for the 36- and 20-mm-id laser tubes are shown in figures 8 and 9. These histograms show the statistical nature of the LDV data. In general, the histograms have an approximately normal distribution with a slight skew to the low-velocity side. The increasing width of the histograms shows an increasing level of turbulence as the side walls are approached. The reported mean velocities were derived from the statistical means of the histograms, and the estimated turbulence levels are based on the statistical standard deviations of the histograms.

Comparison of Pressure and Mass Flow Systems

The pressure and mass flow systems, typically used to estimate the average iodide vapor flow velocity, were compared with the estimated average velocity across the laser tube. (See fig. 10.) The estimated average velocities (tables I and II) were based on the corresponding "pipe factor" multiplied by the LDV mean axial centerline velocities. The "pipe factor" is defined as the average velocity value for the radial distribution of the mean axial velocities divided by the centerline velocity (fig. 11). For the 20- and 36-mm-id laser tubes, the pipe factors were estimated as 0.86 and 0.85, respectively. A linear regression analysis of the results (fig. 10) used

$$\bar{V} = mV_c + b \quad (7)$$

where \bar{V} is the estimated average velocity, V_c is the calculated value using pressure and flowmeter data, m is the slope of the regression analysis, and b is the intercept to show the following:

For the 20-mm-id laser tube,

$$m = 1.00$$

$$b = 0.33$$

$$\text{Correlation coefficient} = 0.999$$

For the 36-mm-id laser tube,

$$m = 1.06$$

$$b = 0.00$$

$$\text{Correlation coefficient} = 0.990$$

The correlation coefficients show that data gave a good straight-line fit. However, the slope of the analysis shows a 6-percent bias between the measured and the calculated values for the 36-mm-id laser tube. In most cases, the calculated velocities were higher than the estimated

average velocities. These differences are attributed mostly to the way that the average velocity was estimated—that is, on an assumed pipe factor and on the LDV mean axial centerline velocity measurements. In summary, estimated average velocities and velocities derived from pressure and mass flow measurements agreed within 6 percent.

Conclusion

Perfluoroalkyl iodide vapor flow-field measurements were made in a continuous wave (cw), solar-simulated, pumped chemical laser system that featured a laser Doppler velocimeter (LDV) system. The measurements were obtained for 20- and 36-mm-id laser tubes under nonlasing conditions. The mean velocity and turbulence-intensity profiles across the laser tube diameter were obtained at different locations. The mean and turbulence-intensity values ranged from 7 to 17 m/sec and 6 to 30 percent, respectively. This study showed that the level of turbulence was higher than generally anticipated. Therefore, modeling of the flow field should include considerations for the effects of turbulence. Findings from the pressure and mass flow instrumentation, normally used to monitor the vapor flow velocity, were compared with data from the LDV. Estimated average velocities, based on LDV mean axial centerline velocities and a corresponding pipe factor, showed that the calculated values for the pressure and mass flow systems agreed within 6 percent. The LDV has provided flow velocity data for calibrating the installed instrumentation and for analyzing the flow characteristics of perfluoroalkyl iodide ($n\text{-C}_3\text{F}_7\text{I}$) vapor inside variously sized laser tubes.

NASA Langley Research Center
Hampton, VA 23681-0001
October 22, 1992

References

1. Lee, Ja H.; Lee, Min H.; and Weaver, Willard R.: High Power CW Iodine Laser Pumped by Solar Simulator. *Proceedings of the International Conference on Lasers '86*, R. W. McMillan, ed., Soc. for Optical & Quantum Electronics, 1987, pp. 150-156.
2. Thompson, H. Doyle; and Stevenson, Warren H.: *Laser Velocimetry and Particle Sizing*. Hemisphere Publ. Corp., c.1979.
3. Gartrell, Luther R.; and Rhodes, David B.: *A Scanning Laser-Velocimeter Technique for Measuring Two-Dimensional Wake-Vortex Velocity Distributions*. NASA TP-1661, 1980.
4. Gartrell, Luther R.; and Jordan, Frank L., Jr.: *Demonstration of Rapid-Scan Two-Dimensional Laser Velocimetry in the Langley Vortex Research Facility for Research in Aerial Applications*. NASA TM-74081, 1977.
5. Young, Warren H., Jr.; Meyers, James F.; and Hepner, Timothy E.: *Laser Velocimeter Systems Analysis Applied to a Flow Survey Above a Stalled Wing*. NASA TN D-8408, 1977.
6. Van de Hulst, H. C.: *Light Scattering By Small Particles*. John Wiley & Sons, Inc., c.1957.
7. Hanson, Steen: Broadening of the Measured Frequency Spectrum in a Differential Laser Anemometer Due to Interference Plane Gradients. *J. Phys. D: Appl. Phys.*, vol. 6, no. 2, Jan. 1973, pp. 164-171.
8. Wang, J. C. F.: Measurement Accuracy of Flow Velocity Via a Digital-Frequency-Counter Laser Velocimeter Processor. *The Accuracy of Flow Measurements by Laser Doppler Methods: Proceedings LDA-Symposium (Copenhagen)*, Technical Univ. of Denmark, 1976, pp. 151-175.
9. Gartrell, Luther R.; Gooderum, Paul B.; Hunter, William W., Jr.; and Meyers, James F.: *Laser Velocimetry Technique Applied to the Langley 0.3-Meter Transonic Cryogenic Tunnel*. NASA TM-81913, 1981.

Table I. Data for Flow System Calibration Using 36-mm-id Laser Tube and n-C₃F₇I

Flowmeter reading	Flow rate, SCCM	Pressure, torr	Calculated velocity, m/sec	Measured mean velocity, m/sec	Estimated average velocity, m/sec
30 000	5400	7.5	9.0	10.8	9.3
28 500	5100	7.5	8.5	9.7	8.3
17 000	3000	7.5	5.1	5.2	4.5
3 000	540	7.5	.9	1.2	1.0
7 000	1260	4.0	3.9	4.6	4.0
13 000	2340	5.0	5.8	6.6	5.7
22 000	3960	6.0	8.2	8.9	7.7
25 000	4500	6.2	9.1	10.0	8.6
32 000	5760	7.8	9.2	10.4	8.9

Table II. Data for Flow System Calibration Using 20-mm-id Laser Tube and n-C₃F₇I

Flowmeter reading	Flow rate, SCCM	Pressure, torr	Calculated velocity, m/sec	Measured mean velocity, m/sec	Estimated average velocity, m/sec
22 200	3996	11.1	14.6	15.9	13.5
19 200	3456	11.1	12.6	13.9	11.8
13 500	2430	11.1	8.9	9.5	8.1
12 000	2160	11.2	7.8	8.7	7.4
11 100	1998	11.2	7.2	8.0	6.8
9 700	1746	11.1	6.4	7.1	6.0
7 200	1296	11.1	4.7	5.4	4.6
4 200	756	13.0	2.3	2.9	2.5

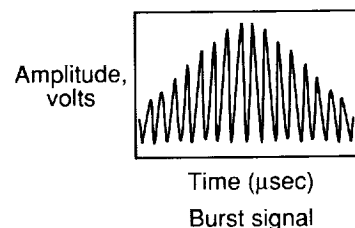
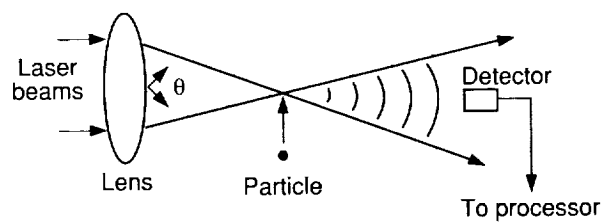


Figure 1. The LDV technique.

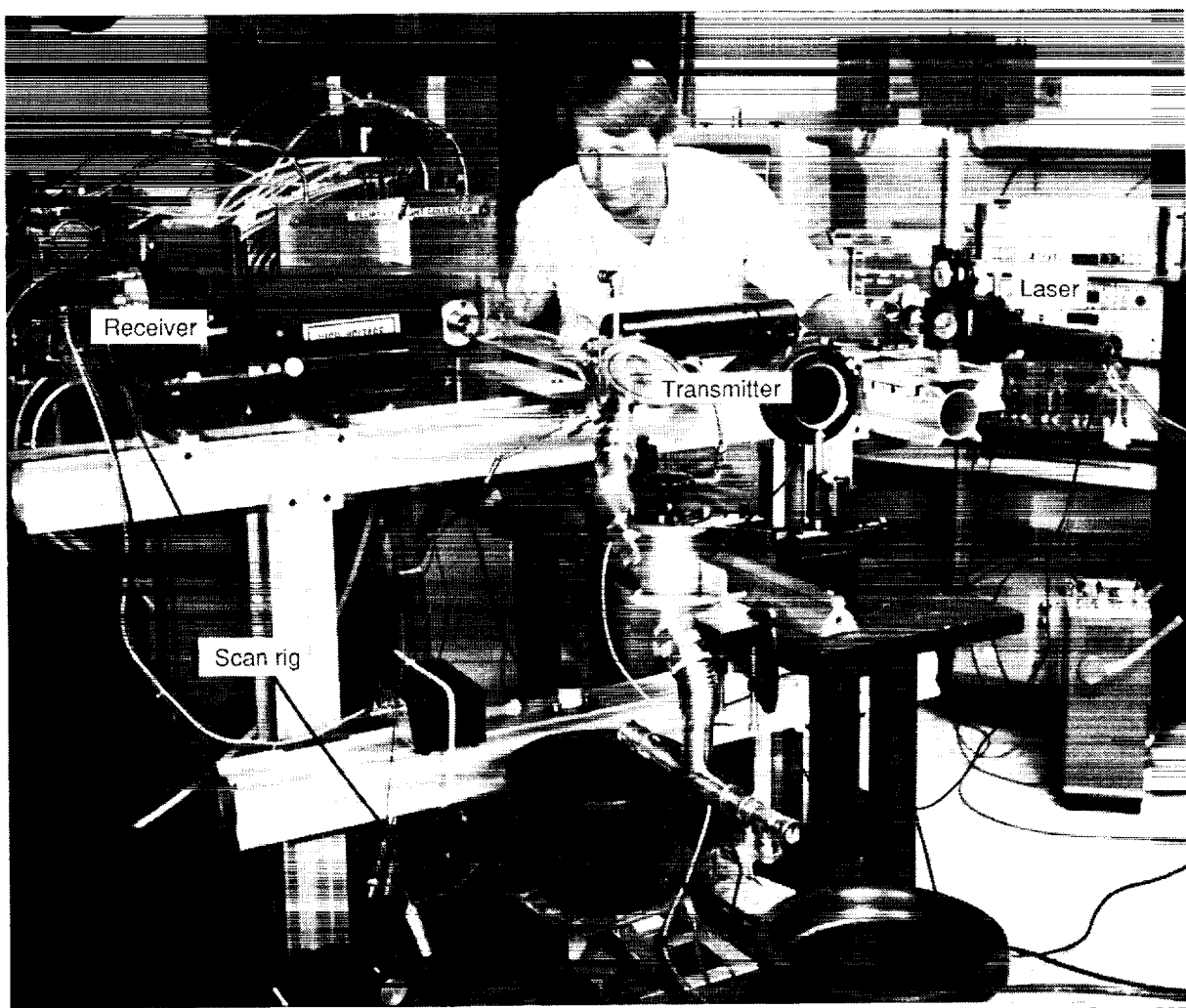


Figure 2. The LDV system mounted on scan rig.

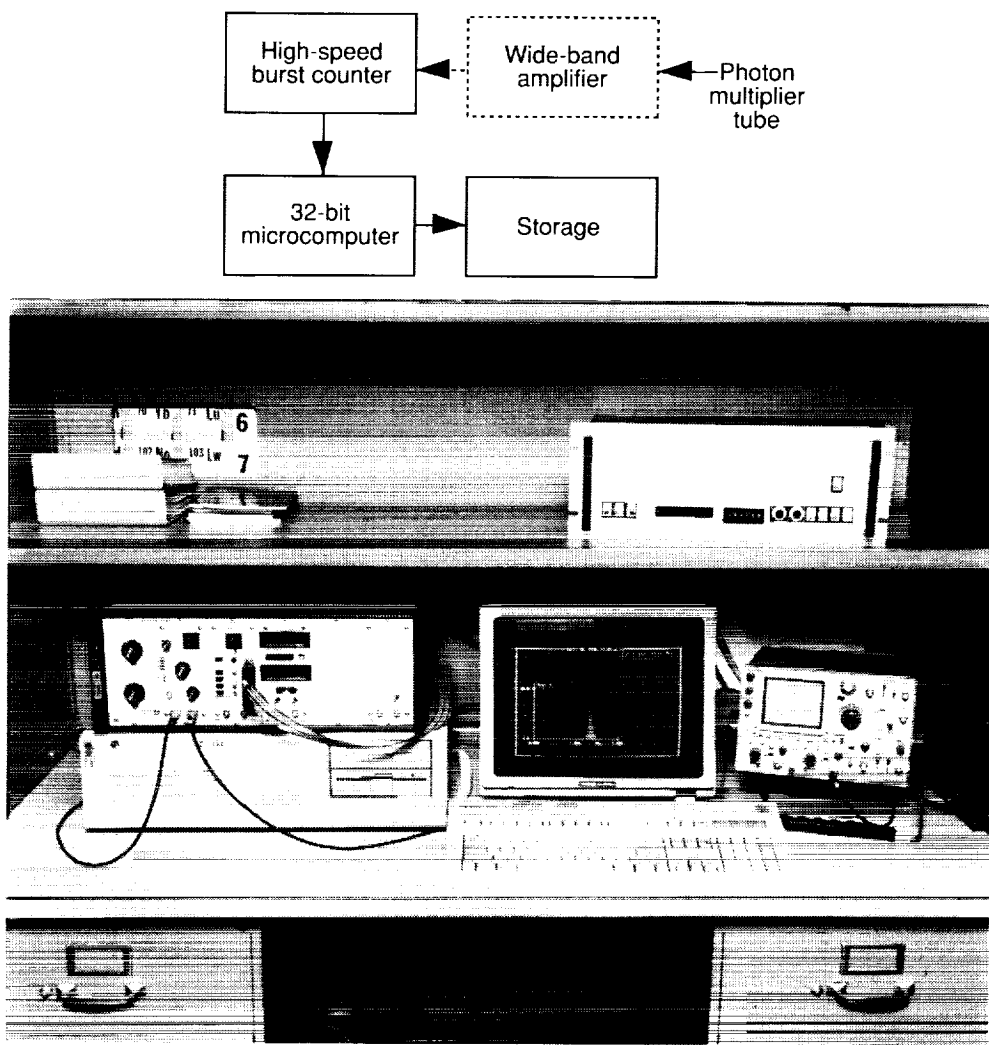


Figure 3. The LDV electronics system.

L-90-4846

ORIGINAL PAGE
BLACK AND WHITE PHOTOGRAPH

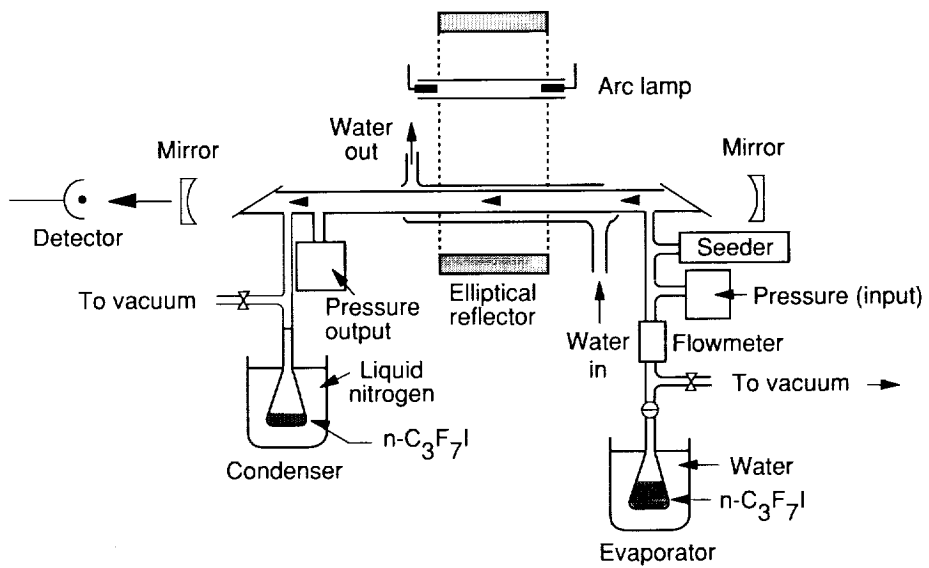


Figure 4. Continuous flow solar-pumped iodide laser system.

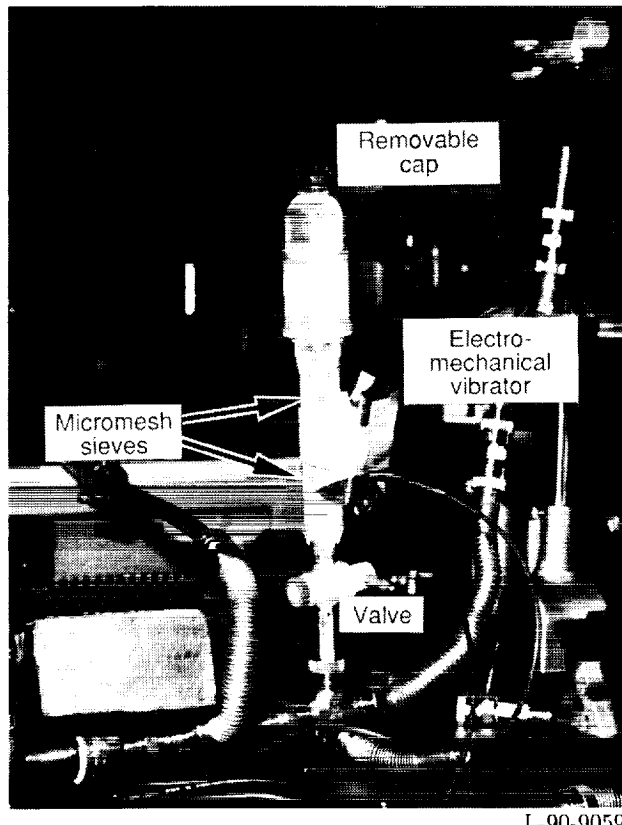
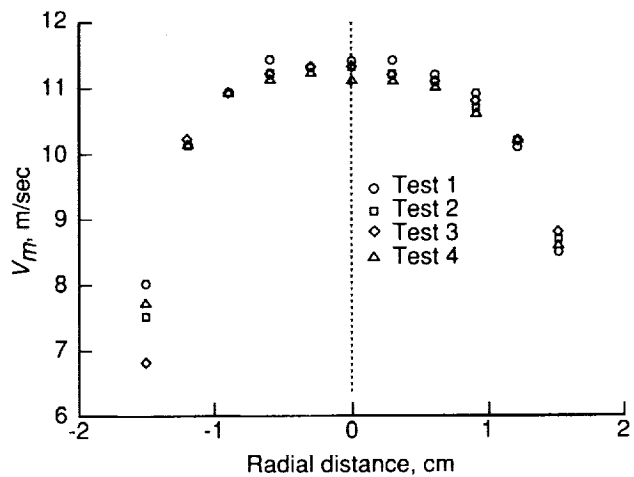
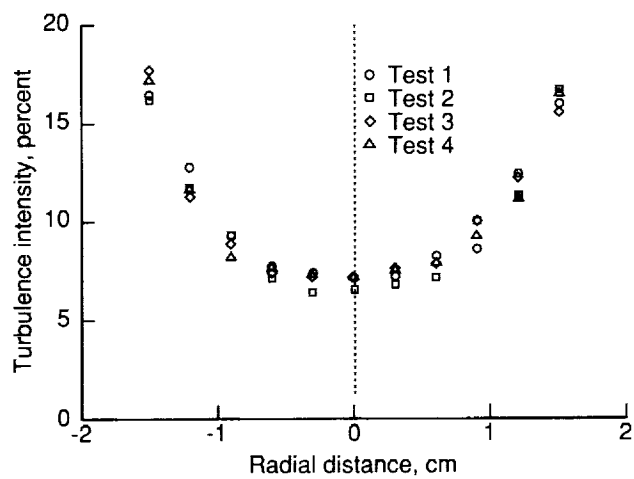


Figure 5. The seeding apparatus.

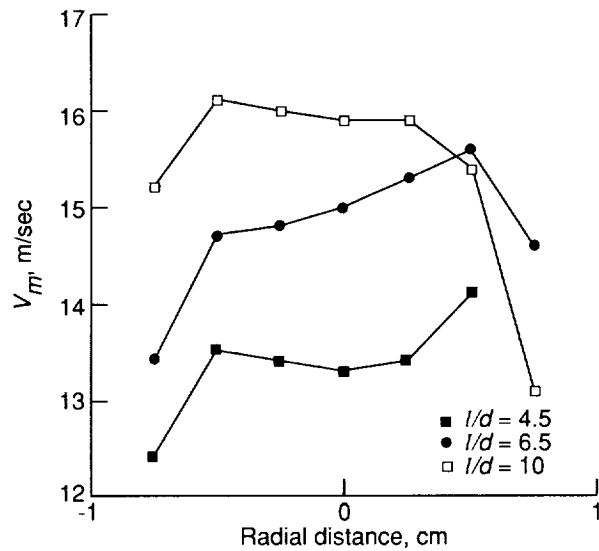


(a) Velocity profile.

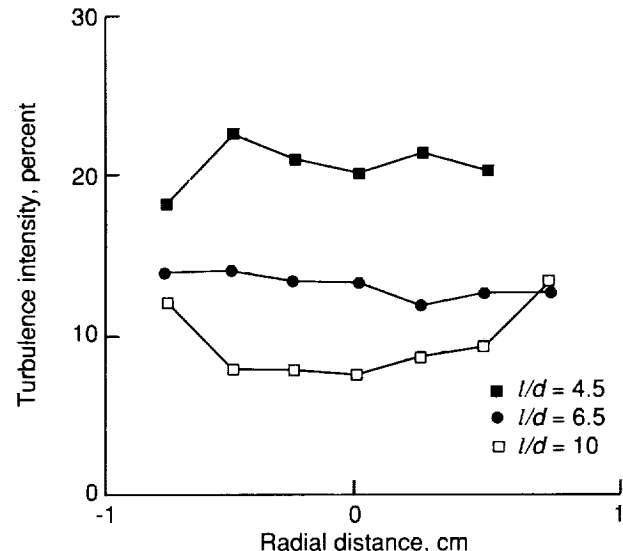


(b) Longitudinal turbulence intensity.

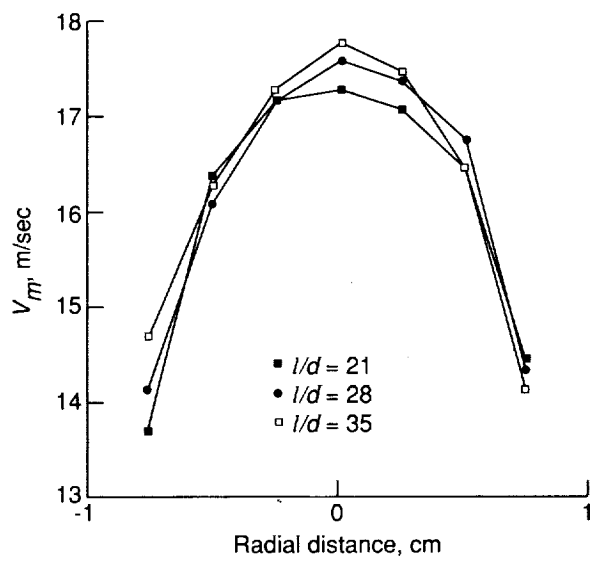
Figure 6. Measurements of LDV in 36-mm-id laser tube at 5 torr and $l/d = 24$.



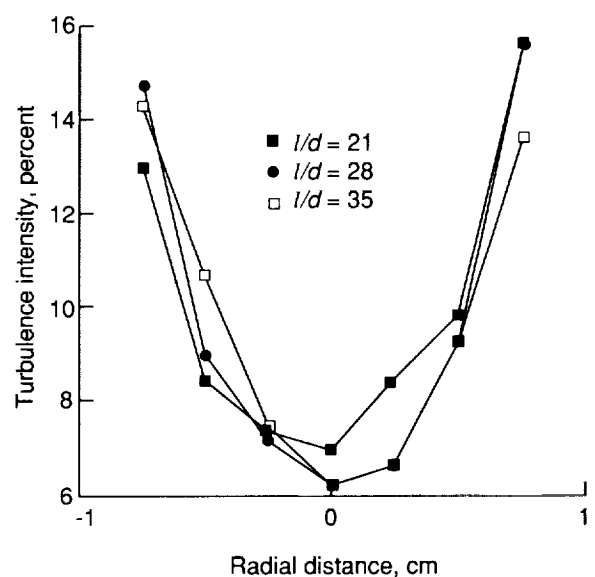
(a) Velocity profile.



(b) Longitudinal turbulence intensity.

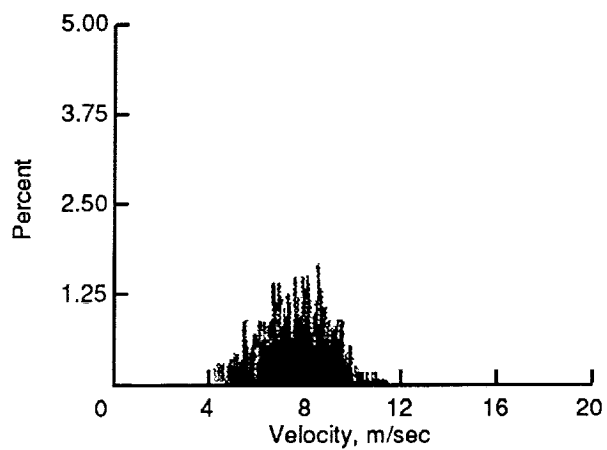


(c) Velocity profile.

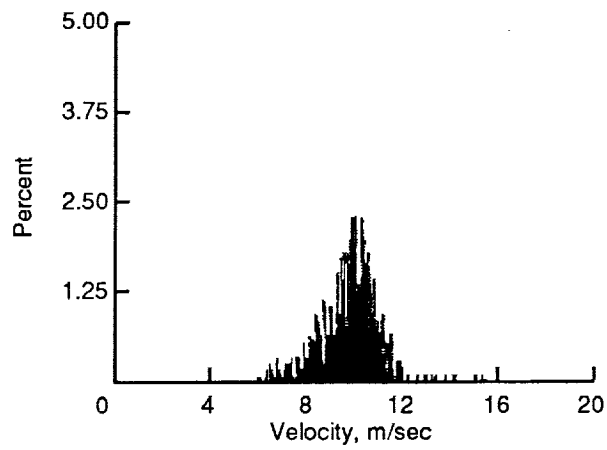


(b) Longitudinal turbulence intensity.

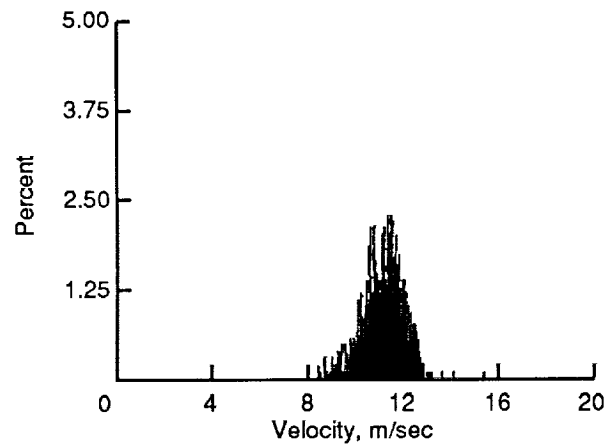
Figure 7. Measurements of LDV in 20-mm-id laser tube at 10 torr.



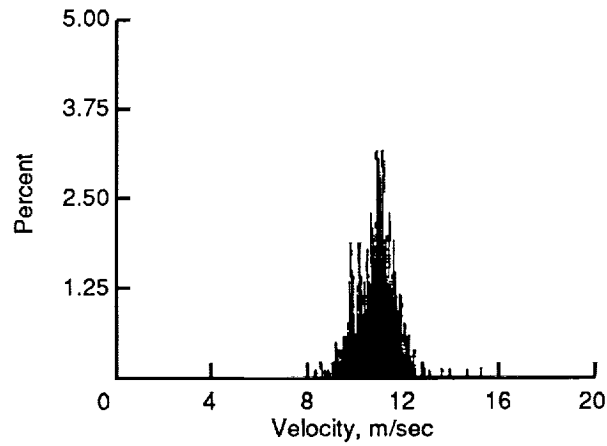
(a) $x = -1.5$ cm.



(b) $x = -1.2$ cm.

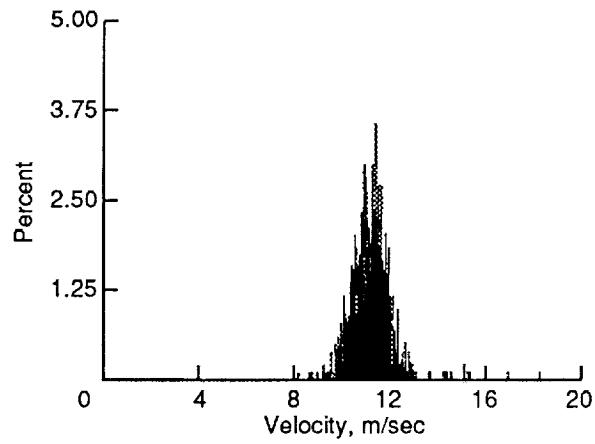


(c) $x = -0.9$ cm.

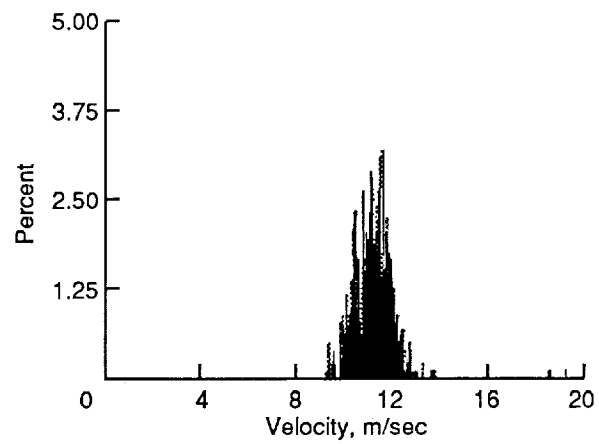


(d) $x = -0.6$ cm.

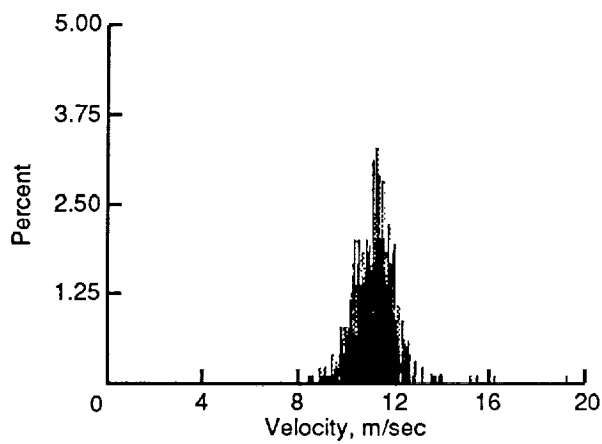
Figure 8. Typical velocity histogram plots for 36-mm-id laser tube at 5 torr and $l/d = 24$.



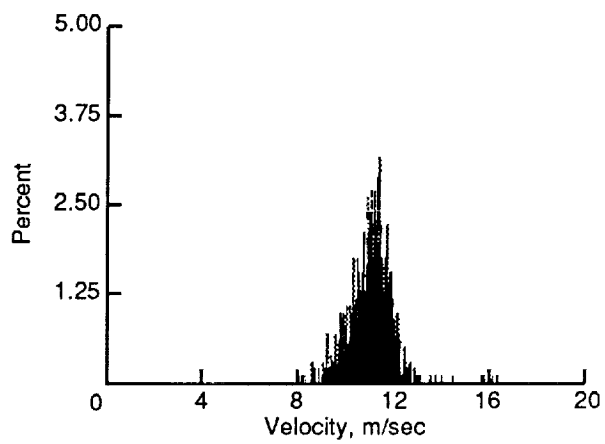
(e) $x = -0.3$ cm.



(f) $x = 0.0$ cm.

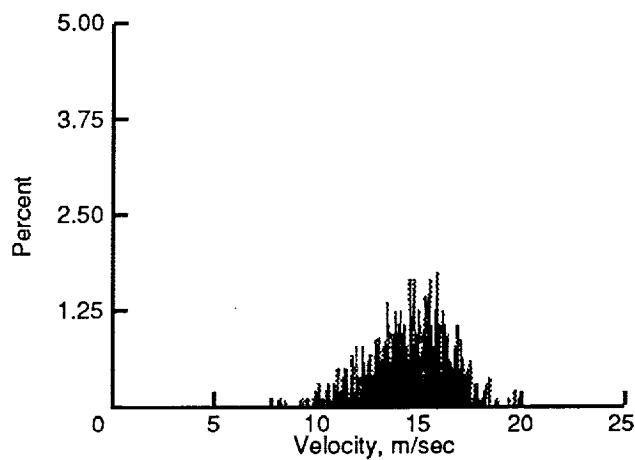


(g) $x = 0.3$ cm.

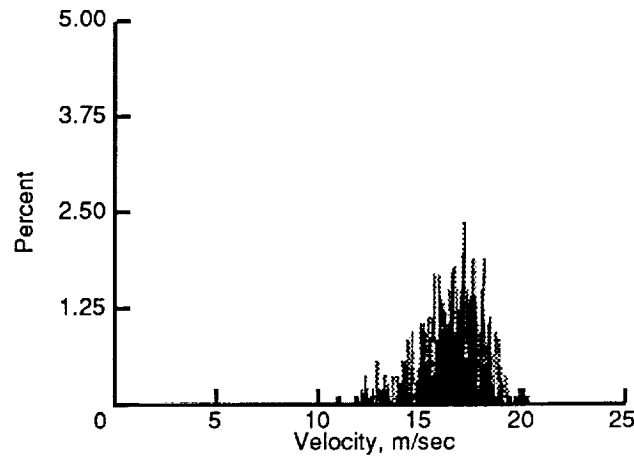


(h) $x = 0.6$ cm.

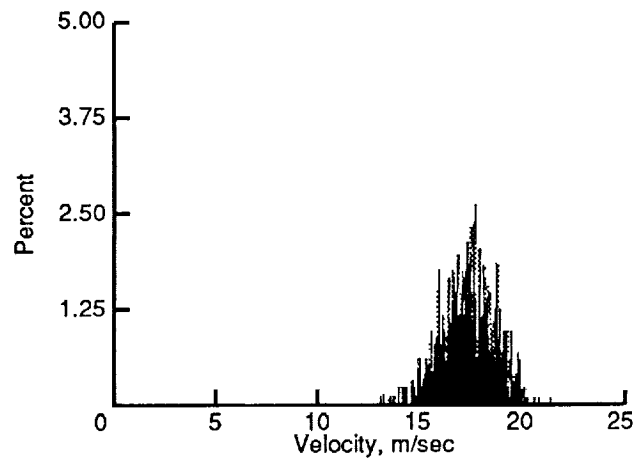
Figure 8. Concluded.



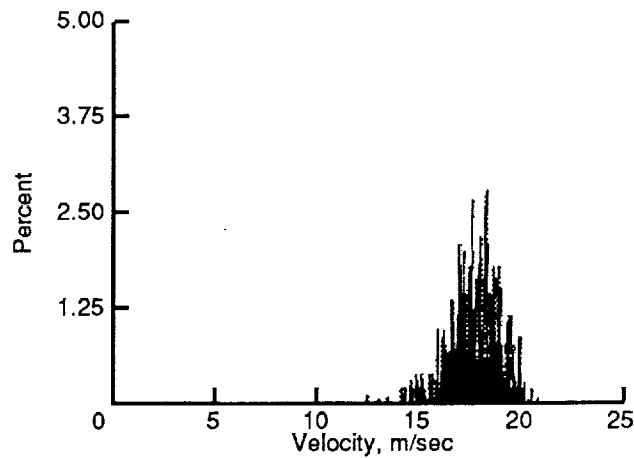
(a) $x = -0.75$ cm.



(b) $x = -0.5$ cm.

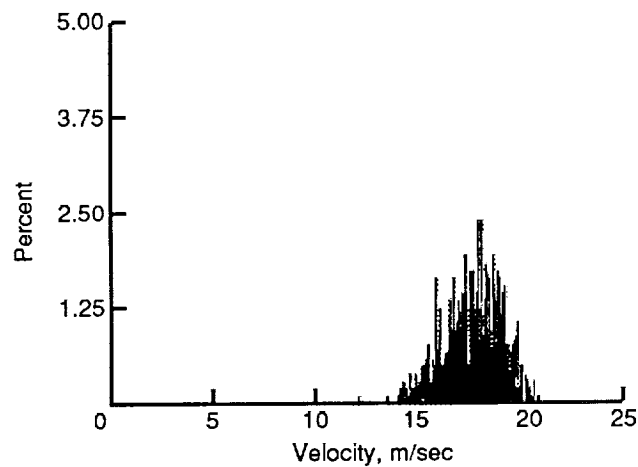


(c) $x = -0.25$ cm.

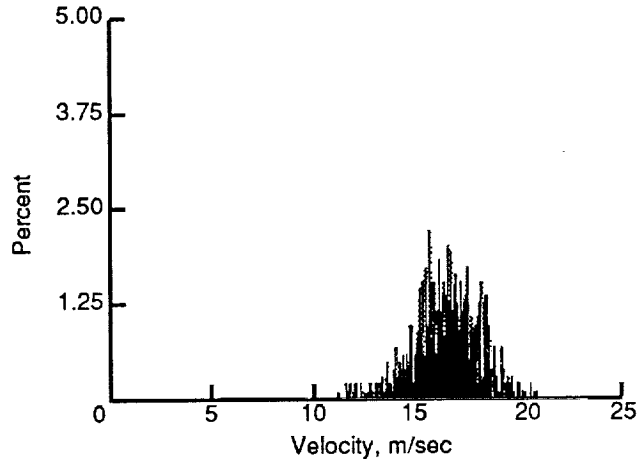


(d) $x = 0.00$ cm.

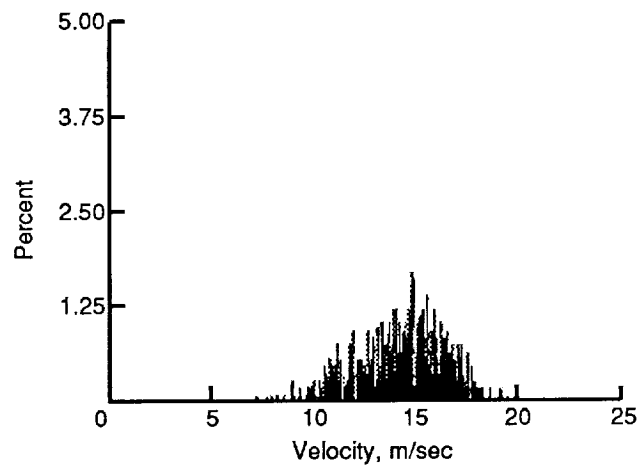
Figure 9. Typical velocity histogram plots for 20-mm-id laser tube at 10 torr and $l/d = 34.75$.



(e) $x = 0.25$ cm.

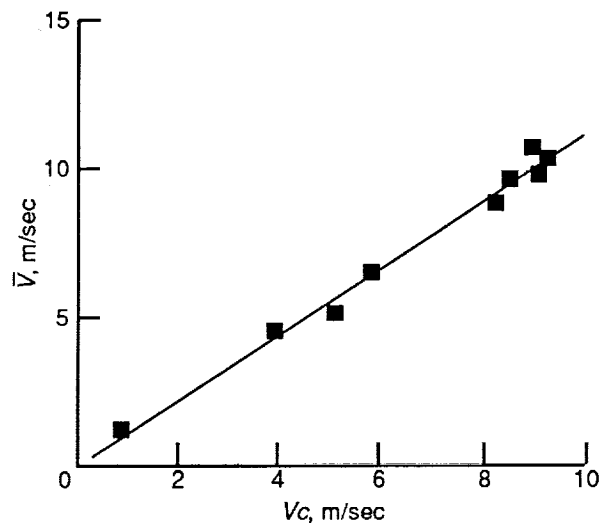


(f) $x = 0.50$ cm.

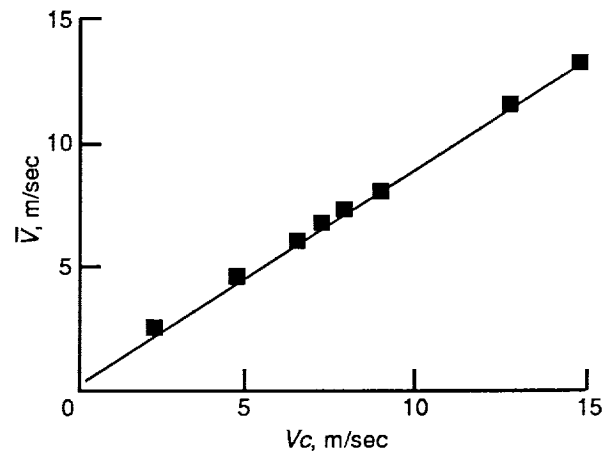


(g) $x = 0.75$ cm.

Figure 9. Concluded.

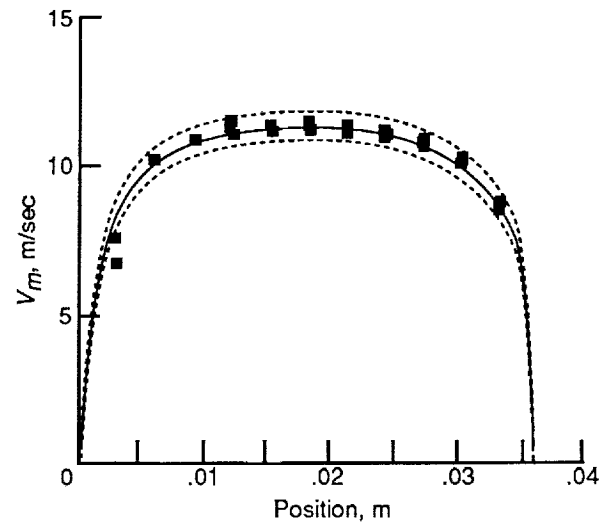


(a) $\bar{V} = 0.86 V_m$; 36 mm id.

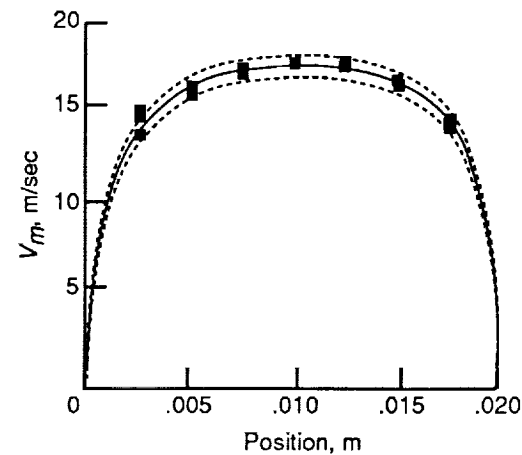


(b) $\bar{V} = 0.85 V_m$; 20 mm id.

Figure 10. Estimated versus calculated velocity for flowmeter calibration.



(a) 36 mm id.



(b) 20 mm id.

Figure 11. Curve-fit plots of LDV mean axial velocity distributions for estimating pipe factor in laser tubes.

REPORT DOCUMENTATION PAGE			Form Approved OMB No. 0704-0188
<p>Public reporting burden for this collection of information is estimated to average 1 hour per response, including the time for reviewing instructions, searching existing data sources, gathering and maintaining the data needed, and completing and reviewing the collection of information. Send comments regarding this burden estimate or any other aspect of this collection of information, including suggestions for reducing this burden, to Washington Headquarters Services, Directorate for Information Operations and Reports, 1215 Jefferson Davis Highway, Suite 1204, Arlington, VA 22202-4302, and to the Office of Management and Budget, Paperwork Reduction Project (0704-0188), Washington, DC 20503.</p>			
1. AGENCY USE ONLY(Leave blank)	2. REPORT DATE	3. REPORT TYPE AND DATES COVERED	
	February 1993	Technical Memorandum	
4. TITLE AND SUBTITLE	Application of Laser Doppler Velocimeter to Chemical Vapor Laser System		5. FUNDING NUMBERS
6. AUTHOR(S)	Luther R. Gartrell, Bagher M. Tabibi, William W. Hunter, Jr., Ja H. Lee, and Mark T. Fletcher		WU 505-59-54-03
7. PERFORMING ORGANIZATION NAME(S) AND ADDRESS(ES)	NASA Langley Research Center Hampton, VA 23681-0001		8. PERFORMING ORGANIZATION REPORT NUMBER
9. SPONSORING/MONITORING AGENCY NAME(S) AND ADDRESS(ES)	National Aeronautics and Space Administration Washington, DC 20546-0001		10. SPONSORING/MONITORING AGENCY REPORT NUMBER
11. SUPPLEMENTARY NOTES Gartrell, Hunter, Lee, and Fletcher: Langley Research Center, Hampton, VA; Tabibi: Hampton University, Hampton, VA.			
12a. DISTRIBUTION/AVAILABILITY STATEMENT Unclassified-Unlimited Subject Category 36		12b. DISTRIBUTION CODE	
13. ABSTRACT <i>(Maximum 200 words)</i> A laser Doppler velocimeter (LDV) system has been used to measure iodide vapor flow fields inside two different-sized laser tubes. Typical velocity profiles across the laser tubes were obtained with an estimated ± 1 percent bias and ± 0.3 to 0.5 percent random uncertainty in the mean values and ± 2.5 percent random uncertainty in the turbulence-intensity values. Centerline velocities and turbulence intensities for various longitudinal locations ranged from 13 to 17.5 m/sec and 6 to 20 percent, respectively. In view of these findings, the effects of turbulence should be considered for flow field modeling. The LDV system provided calibration data for pressure and mass flow systems used routinely to monitor the research laser gas flow velocity.			
14. SUBJECT TERMS Laser velocimeter; Flow velocity measurement; Lasers			15. NUMBER OF PAGES 19
			16. PRICE CODE A03
17. SECURITY CLASSIFICATION OF REPORT Unclassified	18. SECURITY CLASSIFICATION OF THIS PAGE Unclassified	19. SECURITY CLASSIFICATION OF ABSTRACT	20. LIMITATION OF ABSTRACT